Libertas Academica
FREEDOM TO RESEARCH

Open Access: Full open access to this and thousands of other papers at http://www.la-press.com.

Environmental Health Insights

Supplementary Issue: Occupational Health and Industrial Hygiene

Magnetic Resonance Imaging of Graded Skeletal Muscle Injury in Live Rats

Robert G. Cutlip[1], Melinda S. Hollander[2], G. Allan Johnson[3], Brice W. Johnson[4], Sherri A. Friend[5] and Brent A. Baker[5]

[1]West Virginia University, School of Medicine, Morgantown, WV, USA. [2]West Virginia University, Office of Research Integrity and Compliance Morgantown, WV, USA. [3]Duke University Medical Center, Durham, NC, USA. [4]MRPath Inc., Durham, NC, USA. [5]Centers for Disease Control, National Institute for Occupational Safety and Health (NIOSH/CDC), Morgantown, WV, USA.

ABSTRACT

INTRODUCTION: Increasing number of stretch–shortening contractions (SSCs) results in increased muscle injury.

METHODS: Fischer Hybrid rats were acutely exposed to an increasing number of SSCs *in vivo* using a custom-designed dynamometer. Magnetic resonance imaging (MRI) imaging was conducted 72 hours after exposure when rats were infused with Prohance and imaged using a 7T rodent MRI system (GE Epic 12.0). Images were acquired in the transverse plane with typically 60 total slices acquired covering the entire length of the hind legs. Rats were euthanized after MRI, the lower limbs removed, and tibialis anterior muscles were prepared for histology and quantified stereology.

RESULTS: Stereological analyses showed myofiber degeneration, and cellular infiltrates significantly increased following 70 and 150 SSC exposure compared to controls. MRI images revealed that the percent affected area significantly increased with exposure in all SSC groups in a graded fashion. Signal intensity also significantly increased with increasing SSC repetitions.

DISCUSSION: These results suggest that contrast-enhanced MRI has the sensitivity to differentiate specific degrees of skeletal muscle strain injury, and imaging data are specifically representative of cellular histopathology quantified via stereological analyses.

KEYWORDS: MRI, skeletal muscle injury, stretch–shortening contraction, myofiber degeneration, inflammation

SUPPLEMENT: Occupational Health and Industrial Hygiene

CITATION: Cutlip et al. Magnetic Resonance Imaging of Graded Skeletal Muscle Injury in Live Rats. *Environmental Health Insights* 2014:8(S1) 31–39 doi: 10.4137/EHI.S15255.

RECEIVED: June 2, 2014. **RESUBMITTED:** September 12, 2014. **ACCEPTED FOR PUBLICATION:** September 22, 2014.

ACADEMIC EDITOR: Timothy Kelley, Editor in Chief

TYPE: Original Research

FUNDING: This study was supported by Internal NIOSH funds. The Duke Center for *In Vivo* Microscopy (GAJ) is supported by NIH/NIBIB P41 EB015897. The authors confirm that the funder had no influence over the study design, content of the article, or selection of this journal.

DISCLAIMER: The findings and conclusions in this report are those of the authors and do not necessarily represent the views of the NIOSH.

COMPETING INTERESTS: All authors disclose no potential conflicts of interest.

CORRESPONDENCE: bwb3@cdc.gov

Paper subject to independent expert blind peer review by minimum of two reviewers. All editorial decisions made by independent academic editor. Upon submission manuscript was subject to anti-plagiarism scanning. Prior to publication all authors have given signed confirmation of agreement to article publication and compliance with all applicable ethical and legal requirements, including the accuracy of author and contributor information, disclosure of competing interests and funding sources, compliance with ethical requirements relating to human and animal study participants, and compliance with any copyright requirements of third parties. This journal is a member of the Committee on Publication Ethics (COPE).

Introduction

Contraction-induced skeletal muscle injury is clinically diagnosable as a strain injury, with the degree of soft-tissue injury proportional to the severity of the diagnosed strain, and this is a highly prevalent condition observed in orthopedics;[1] resulting from various etiologies incurred ubiquitously across all domains (ie, occupational, athletic, military, aging, etc.). Indeed, overt soft-tissue injury (specifically that of skeletal muscle resulting in a musculoskeletal disorder/disease – MSD) resulting from single and repeated mechanical loading exposures is prevalent in the workplace and accounts for ~38% of all medically diagnosed injuries.[2] This leads to a significant increase in lost workdays and increased disability costs.[3] The United States Bureau of Labor Statistics (BLS),[4] which defines MSD, based strongly on mechanism of injury, to "*include cases where the nature of the injury or illness is sprains, strains, tears, back pain, hurt back; soreness, pain, hurt except the back; carpal tunnel syndrome, hernia, or musculoskeletal system and connective tissue diseases and disorders, when the event or exposure leading to the injury or illness is bodily reaction/bending, climbing, crawling, reaching, twisting, overexertion, or repetitive.*" Specific examples of occupationally induced and athletically induced MSD

would be a hamstring (biceps femoris) muscle, strain induced by overextension of the active muscle, while an external load is being displaced/resisted by a worker or the same injury in an athlete who actively resists/displaces an externally applied force when attempting to perform a deadlift exercise.

Even though most models of contraction-induced skeletal muscle injury exclusively use lengthening ("eccentric") contractions to induce soft-tissue trauma, a more physiologically relevant contraction paradigm will incorporate both isometric and shortening ("concentric") contractions along with lengthening contractions. This contraction paradigm is the basis of the stretch–shortening cycle (isometric–lengthening–shortening) or stretch–shortening contraction (SSC), which physiologically is the most representative movement pattern in humans and other mammals.[5,6] Thus, the use of controlled muscle contractions is the most beneficial way to study skeletal muscle injury and repair mechanisms, and how they relate to work-related MSDs.[35,36] Indeed, findings from volitional animal models of repetitive motion,[7] human models of electrically evoked exercise overload,[8] and electrically evoked rat dynamometer models[9–12] demonstrate that the cellular pathways of inflammation, degeneration, and regeneration and the accompanying histopathology and biomechanical decrements are congruent. It is also accepted that the amount of mechanical loading comprising eccentric contractions has been shown to have a graded effect on both changes in muscle performance and the extent of myofiber injury.[6,11]

Thus, our understanding of the onset of events initiating contraction-induced muscle injury may be broadened by implementing more rigorous morphological and biochemical analyses of the targeted muscle tissue.[9,10,13–15] Studies of soft-tissue injury resulting from acute strain overload have been conducted using animal[9–11,16–18] and human models;[19,20] and to date, the vast majority of these studies have utilized histopathology or biomechanical performance as a means to quantify contraction-induced muscle injury. Yet, clinical diagnosis of soft-tissue injury relies more on imaging techniques that include magnetic resonance imaging (MRI), which tend to evaluate and "rule-out" muscle ruptures.[21] Utilizing this approach, animal studies have shown that MRI can reliably be used to illustrate changes in soft-tissue in general, but little is known as to how cellular events are representative of specific myofiber injury processes following graded injury perturbations.[22,23] As important, no studies have investigated the exposure–response continuum and the effect of increasing repetition number of injurious SSCs *in vivo*, and whether MRI findings in live animals are representative of the quantitative degree of skeletal muscle injury at the anatomical/cellular level.

The specific purpose of the current study was to investigate if and how contrast-enhanced MRI was representative of histopathological findings that previously have been shown to be concomitant with decreased performance in rats following electrically evoked (supramaximal), injurious SSCs *in vivo*.[6] The specific aims of the current study were two-fold: (1) investigate the effects that increasing SSC repetition number has on MRI signal intensity and the affected soft-tissue area 72 hours following an acute, injurious session of SSC in live rats, and (2) compare the response from MRI results to histopathological findings using a standard stereological technique previously developed in our lab;[9] the latter completed post sacrifice. Specifically, we hypothesized that rats loaded with increasing numbers of SSCs will have increased MRI signal intensity and that the affected area constituting skeletal muscle injury will also be increased, and that this will be representative of changes in stereological indices of myofiber degeneration, cellular infiltrates (ie, inflammatory cells) and non-cellular infiltrates (ie, edema), and normal myofibers 72 hours following injurious SSC loading.

Materials and Methods

Experimental animals. Young, male (12 weeks, $N = 12$; $n = 3$ per group) Fischer 344 × Brown Norway (F344xBN) rats were used in the present study. The F344xBN rats were selected for this study because our future research plans are to investigate the effects of muscle injury and the potential for *in vivo* imaging (as well as other potential modalities) in aged rats; and thus, this strain of rats is the approved National Institute for Aging (NIA) rodent model. Rats were housed in AAALAC accredited animal quarters, where the temperature and light/dark cycle (dark cycle from 7:00 AM to 7:00 PM) were controlled, and food and water were provided ad libitum. All rats were exposed to a standardized experimental protocol approved by the NIOSH Animal Care and Use Committee that complied with the Guide for the Care and Use of Laboratory Animals. Rats were randomized to groups exposed to either 0 (isometric control), 30, 70, or 150 SSCs *in vivo* using a custom-designed dynamometer with a 72-hour recovery. The right, contralateral limb from each animal served as an intra-animal control (CON group).

Experimental setup. Animals were tested on a custom-built rodent dynamometer as previously described.[24] Rat dorsiflexor muscles were exposed to a SSC protocol as previously described.[6] Briefly, as illustrated in Figure 1A and 1B, rats were anesthetized with isoflurane gas in an "induction" tank (Surgivet Anesco Inc.), placed supine on a heated *x–y* positioning table of the rodent dynamometer, with an anesthetic mask over the nose and mouth of the animal. The knee was secured with a knee holder, and the left foot (loaded limb) was secured in the load cell fixture with the ankle axis (assumed to be between the medial and lateral malleoli aligned with the axis of rotation of the load cell fixture). Each animal was monitored during the procedure to maintain proper anesthetic depth and body temperature.

Functional testing. Platinum stimulating electrodes (Grass Medical Instruments) were placed subcutaneously to span the common peroneal nerve. Activation of the electrical stimulator (Grass Stimulator, Astro-Med Inc., Grass Instrument Division; Model # SD9J) resulted in muscle contraction of the dorsiflexor

muscle group. Stimulator settings were optimized to maximize dorsiflexor contractile performance as previously described.[11] Muscle stimulation for all protocols was conducted at 120 Hz stimulation frequency, 0.2 milliseconds pulse duration, and 4 V magnitude. The joint angle of the rat ankle was defined as the angle between the tibia and the plantar surface of the foot. The angular position of the load cell corresponded to the foot position. Vertical forces produced by the dorsiflexor muscles at the interface of the aluminum sleeve fitted and the dorsum of the foot was measured via a load cell transducer (Sensotec Inc.). An isometric contraction was performed at 90° ankle angle using 300 milliseconds simulation duration. An isometric contraction was performed 2 minutes (min) preceding (pre) and 2 minutes following (post) either 3 sets of 10 SSC repetitions (30R), 7 sets of 10 SSC repetitions (70R), 15 sets of 10 SSC repetitions (150R), or 15 isometric contractions (0 group), and 72 hours post-SSC exposure (immediately prior to the animal being euthanized). All animals were returned to their home cages in the animal quarters after their respective treatment protocol and remained there with access to food and water ad libitum until time of sacrifice. Animals were monitored after their treatment exposure and did not show any signs of distress.

Injury protocol. Activation of the dorsiflexor muscle group (including the tibialis anterior [TA] muscle) was achieved via electrically evoked (supramaximal) stimulation of the common peroneal nerve of the left limb for 100 milliseconds. Movement of the load cell fixture then commenced from 90° to 140° angular position at a velocity of 500°/second, in a reciprocal fashion for 10 oscillations. After 10 oscillations, the load cell fixture was stopped at 90° and the dorsiflexor group was deactivated 300 milliseconds later. The total stimulation time per set was 2.8 seconds. The sets of repetitions were conducted at 2-minute intervals.

MRI imaging. Rats were anesthetized 72 hours after mechanical loading exposure, infused with Prohance (Bracco Diagnostics Inc., Princeton, NJ, USA), and then imaged immediately using a 7T/210-mm horizontal bore Magnex magnet interfaced to a GE EXCITE (GE Epic 12.0) imaging console modified for small animal imaging. Magnex gradients with a clear bore of 120 mm provided encoding gradients of up to 400 mT/m with rise times <200 microseconds. Images were acquired using a multi-slice spin echo sequence with TR = 900 milliseconds, TE = 10 milliseconds, 1-mm slice, 512 × 512 encoding matrix, one excitation per view yielding in-plane spatial resolution of 117 × 117 microns (MRPath Inc.). Images were acquired in the transverse plane with typically 60 total slices covering the entire length of the hind legs. A standard clinical contrast agent (Magnevist – gadopentetate dimeglumine, Berlex/Bayer Health Care) was administered via tail vein at a concentration of 0.2 mmol/kg similar to the method published by Amthor and colleagues.[25] Rats were euthanized after imaging and the lower limbs were removed and placed in formalin. The TA muscles were prepared for histological analyses using standard hematoxylin and eosin staining and quantified using a standardized and established stereological technique.[9,10] MRI images were quantified using a damage index consisting of the percentage of tissue area disruption in the TA and image contrast (signal intensity) using a mean area gray value (mArGV). MRI images were processed using Optimas software (Meyer Instruments Inc., Houston, TX, USA).

Myofiber definitions. Stereology was used to quantify the degree of myofiber degeneration, and the accompanying changes in the interstitial space in the TA muscle from each group. Myofibers have been defined previously,[9,10] but briefly: normal myofibers demonstrated: (1) complete contact with adjacent myofibers, (2) a smooth outer membrane, and (3) no presence of internal inflammatory cells. Degenerative myofibers displayed: (1) a loss of contact with adjacent myofibers, (2) presence of internal inflammatory cells, and (3) an outer membrane interdigitated with inflammatory cells.

Stereology. Quantitative morphometric methods were used to measure the volume fraction, surface densities, and average thickness of normal myofibers, degenerative myofibers, and the interstitial space as previously described.[6,9,10] The interstitium was divided into the endomysium and the perimysium space, which included capillaries. Stereology was also used to quantify the degree of inflammation, which was quantified as either non-cellular interstitium (NCI) indicative of edema or cellular interstitium (CI); CI consisted of all possible infiltrating cells such as, but not limited to, inflammatory, endothelial, and fibroblasts. A stage micrometer was used to identify the midpoint of the sample section. Point and intercept counts using a 121 point/11 line overlay graticule (12.5-mm square with 100 divisions) at 40× magnification were taken at five equally spaced sites across the section. This process was repeated, 2 mm on either side of the midpoint of the section for a total of 1210 points and 110 intercept lines per section. Volume density or the percent (%) tissue volume was computed from the percentage of points over the tissue section to points over normal myofibers, degenerative myofibers, CI, and NCI. Because of the nature of the infusion technique (and the likelihood of overestimating the volume density of the non-cellular component of the interstitial space), NCI was not quantified as has been customarily reported.[6] Intercepts over the line overlay were counted for the perimeter of normal myofibers, degenerative myofibers, and interstitium to myofiber transitions. Points and intercepts over blood vessels greater than 25 µm in diameter were excluded. Average thickness or average distance was computed from two times the ratio of volume to surface density according to standard morphometric analysis.[26]

Statistical analysis. Statistical analyses were conducted using SAS Version 8 (SAS Institute). Stereological measurements of the volume and thickness of cellular and non-cellular components were analyzed using two-way (treatment × limb) ANOVAs with the animal as the random factor accounting for measures in both limbs. Post-hoc comparisons were made using Fisher's Least Significant Difference (LSD) tests. Data for the measurement of the percentage of volume density and

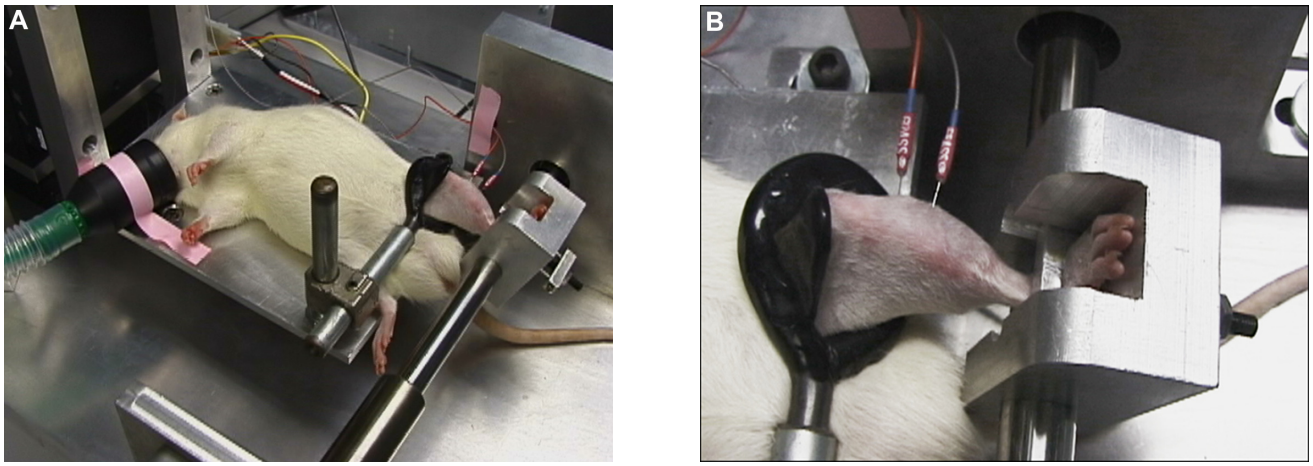

Figure 1. Dorsiflexor muscles were tested on a custom-built rodent dynamometer. (**A**) The knee was secured in flexion (at 90°) with a knee holder with the rodent under anesthesia. (**B**) For each repetition, muscles were fully activated via platinum electrodes spanning the common peroneal nerve, and the load-cell recorded reactive forces in real-time.

average thickness of degenerative myofibers was regarded as ordinal, so a non-parametric Kruskal–Wallis test was applied, and when differences were statistically significant, a Mann–Whitney *U*-test was performed. One section per animal with six animals per group was evaluated and the results were expressed as mean ± S.E.M. Pearson product correlations were performed to analyze relationships between stereological indices of histopathology and MRI signal intensity.

Results

MRI affected area. Sequential, representative MRI images are illustrated in Figure 2A–C, while individual, representative MRI images are illustrated in Figure 3A–C. Figure 4 illustrates the increase in the MRI% affected area for TA muscles of rats loaded with 30R, 70R, and 150R, which had affected areas of 30.84 ± 0.69%, 60.47 ± 1.47%, and 66.98 ± 1.04%, respectively. No affected area was evident in the CON group or the right, contralateral control limb from each animal. Thus, as repetitions of SSCs were increased, a statistically significant increase in the % area of contrast signal intensity relative to the TA muscle area was observed.

MRI signal intensity. Figure 5 illustrates that TA muscles from rats exposed to 30R, 70R, and 150R had mArGV of 47,145.4 ± 1088.6, 51,667.0 ± 1075.5, and 53,324.7 ± 1520.3, respectively. The 70R group exhibited an increased signal intensity compared to the 30R group; however, the 150R group was not statistically different than the 70R group (Fig. 3). All other pairwise comparisons were not statistically different.

Histopathology and stereological indices of myofiber degeneration and inflammation. Figure 6A–E illustrates micrographs from control and SSC injured TA muscles. Figure 7 shows that the percent volume fraction of degenerative myofibers in the exposed TA muscles was 0%, 2.31 ± 1.17%, 9.09 ± 1.6%, and 14.91 ± 2.10%, respectively, for the CON (no difference with the 0 SSC group, data not reported), 30R, 70R, and 150R groups. The percent volume fraction of degenerative myofibers increased significantly as the SSC repetition number increased; however, there was no statistical difference in the percent volume fraction of degenerative myofibers between the 30R and CON group. The percent volume fraction of CI was 1.70 ± 0.13%, 2.53 ± 0.37%, 7.87 ± 1.00%, and 10.61 ± 2.10%, respectively, for the CON (no difference with the 0 SSC group, data not reported), 30R, 70R, and 150R groups. The CON and 30 SSC groups were not significantly different and exhibited less CI than the 70R and 150R groups. Normal myofibers were significantly decreased in the 150R group. All other pairwise comparisons were not statistically different.

Relationship between stereological indices of histopathology and MRI signal intensity. Pearson product correlations were conducted between MRI signal intensity and percent volume fraction of normal myofibers, MRI signal intensity and percent volume fraction of degenerative myofibers, and MRI signal intensity and percent volume fraction of CI. Very strong and significant positive correlations were observed between MRI signal intensity and percent volume fraction of degenerative myofibers (R = 0.97, P = 0.004), respectively, and MRI signal intensity and percent volume fraction of CI (R = 0.98, P = 0.003), respectively.

Discussion

Clinically, MRI is accepted as a valuable tool for the evaluation and confirmation of soft-tissue pathology; yet, how MRI estimates anatomical/cellular "injury" that is reflected by changes in the actual cellular histopathology of the affected soft tissue is not obvious; and furthermore, there are no compelling investigations that have previously established an exposure–response continuum with respect to increasing number of injurious SSCs. In the current study, the two most

significant findings were that: (1) increasing the number of SSCs resulted in increased MRI signal intensity (mArGv) and the percent affected area and (2) this was representative of increasing quantitative morphological indices of CI (indicative of inflammatory cells) and degenerative (necrotic) myofibers. The morphological results were obtained using a systematic sampling technique (stereology) that is rapid and extremely sensitive (a major advantage), and this technique is quite distinct from the approaches previously used to quantify muscle injury.[6,9,10]

Interestingly, the contrast-enhanced MRI results revealed a significant increase in the percent affected area and MRI signal intensity following 30 injurious SSCs compared to the unperturbed, contralateral control muscle. Specifically, both the CI and degenerative myofiber response was significantly increased following 70 SSCs (compared to the 30 SSC group), as this may indicate that the TA's safety threshold (soft tissue tolerance) had been exceeded. While there were no significant cellular infiltrates or myofiber degeneration observed in the contralateral control group and the isometric control group, the

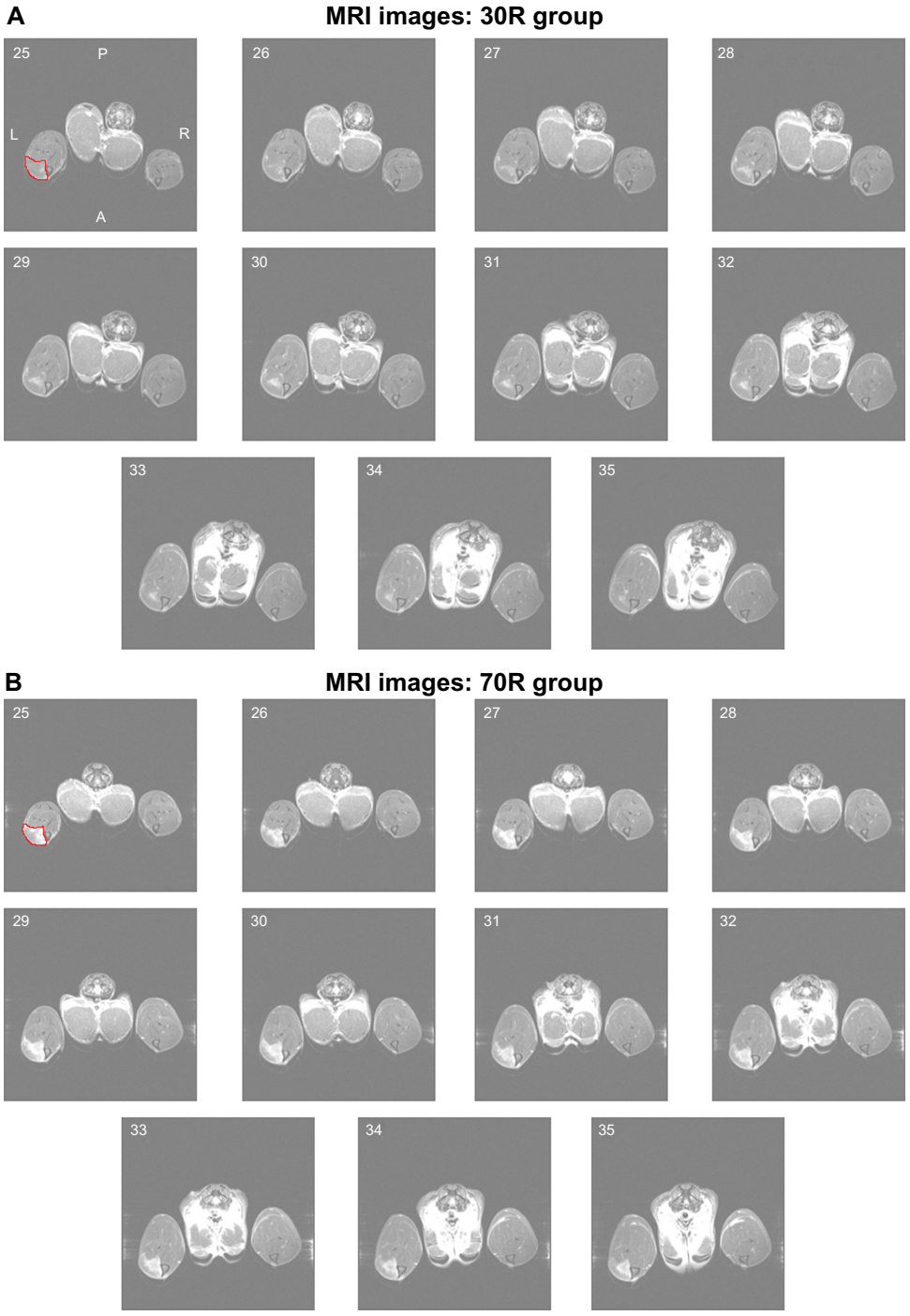

Figure 2. (*Continued*)

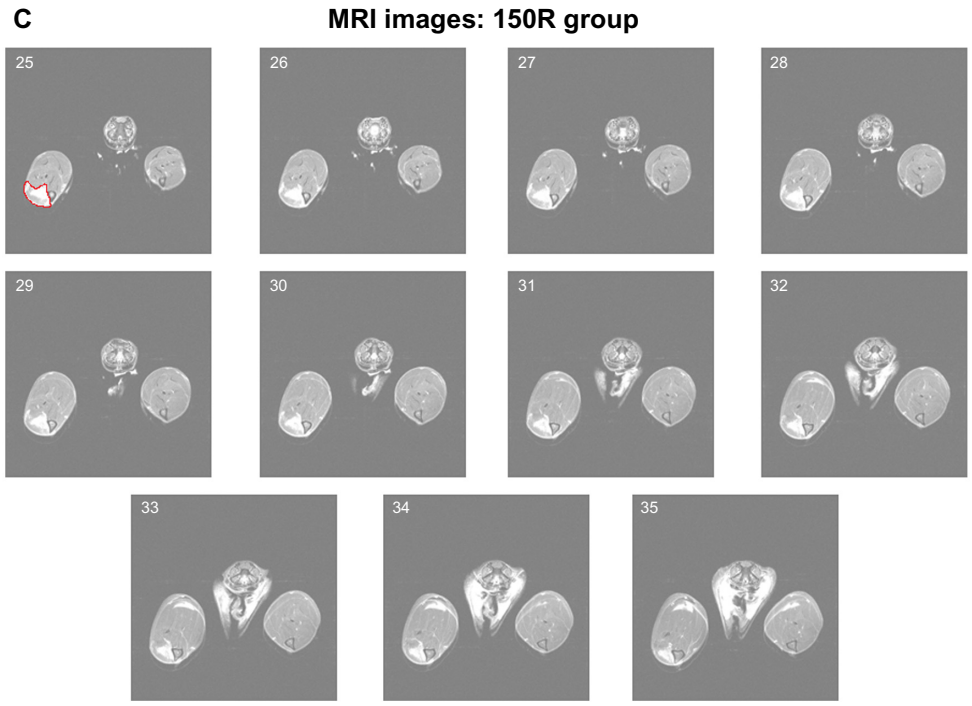

Figure 2. Eleven sequential, representative MRI images in the transverse plane of the contralateral lower limb on the right and the exposed limb on the left after exposure to 30R (**A**), contralateral lower limb on the right and the exposed limb on the left after exposure to 70R (**B**), and contralateral lower limb on the right and the exposed limb on the left after exposure to 150R (**C**). Anatomical orientation is as follows: anterior (A), posterior (P), left (L), and right (R), and the affected area is encircled in red in the first image of each series.

30R group responded with minimal histopathological indices of degenerative myofibers (only one animal in this group had degenerative myofibers present). Our results are in agreement with previous results reported by Geronilla and colleagues and Baker et al using the SSC injury model,[11] and extend their initial observations that myofiber necrosis and myositis increased with increasing SSC repetition number. Additionally, considering that the current study utilized the F344xBN Hybrid rat model compared to previous investigations from our lab using the Sprague-Dawley rat model,[6] we observed consistency across strains with respect to the physiological response of increasing quantity of degeneration and inflammation with increasing SSC number via stereological quantification, and this increase clearly exhibits an exposure–response finding similar to other previous studies.[27] The consistency of these cellular findings suggests that the non-invasive MRI approach may have application in MSD research in aging populations.

The paramagnetic features of Magnevist – gadopentetate dimeglumine – were well suited for visualization of skeletal muscle injury as well as indicative of histopathological

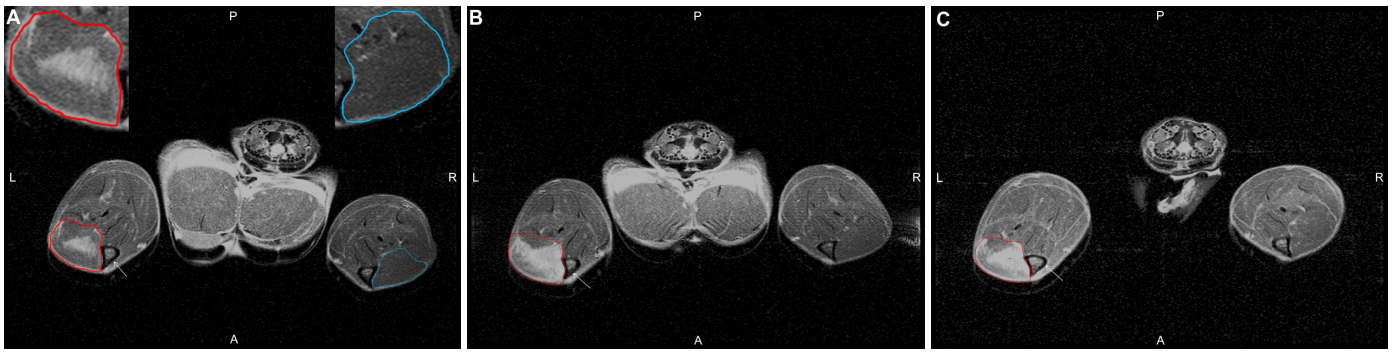

Figure 3. A single representative MRI image in the transverse plane of the contralateral lower limb on the right and the exposed limb on the left after exposure to 30R (**A**), contralateral lower limb on the right and the exposed limb on the left after exposure to 70R (**B**), and contralateral lower limb on the right and the exposed limb on the left after exposure to 150R (**C**). Anatomical orientation is as follows: anterior (A), posterior (P), left (L), and right (R). Left injured limb encircled in red and the right uninjured limb encircled in blue; insets are of the specific dorsiflexor compartment.

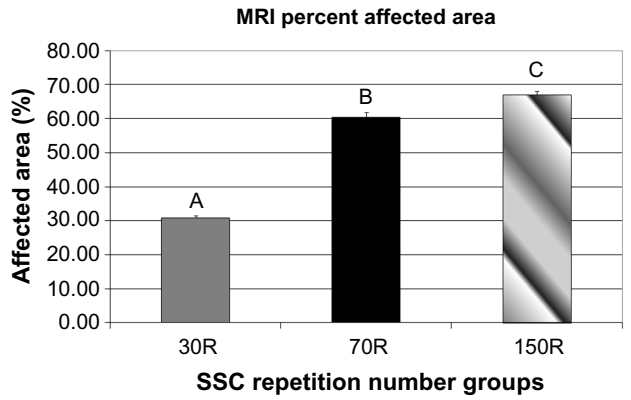

Figure 4. Affected area of the TA muscle after exposure to 30R, 70R, and 150R as a percent of the total area. Different letters denote statistical significance with respect to each SSC exposure group at the $P < 0.05$ level.

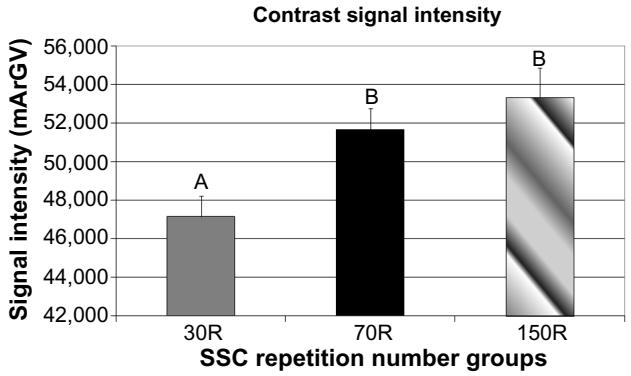

Figure 5. MRI image contrast intensity of the TA muscle from animals exposed to 30R, 70R, and 150R. Different letters denote statistical significance (**A** is different from **B** and **C**, **B** is different from **A** and **C**) with respect to each SSC exposure group at the $P < 0.05$ level.

injury. Specifically, the contrast agent accumulated in the area of injured myofibers and responded in a dose-dependent manner. Moreover, as the number of SSC repetitions was increased, concomitant skeletal muscle injury increased, as did the amount of contrast agent penetrating into the injured myofibers; as such, the contrast intensity and area of contrast increased with increasing SSCs. This finding was similar to the work conducted by Amthor et al and corroborates their previous work.[25]

Concern about using native MRI has been the inability to distinguish between inflammation, edema, fat deposits, and necrotic myofibers. The signal-to-noise ratio of the gadolinium contrast agent was appealing as it did increase in its percent area as well as increase in its signal intensity as the number of SSCs was increased within the perturbed TA tissue. These increases paralleled the histopathological findings in the injured TA tissue, which quantified changes in degenerative myofibers, cellular components of inflammation, and non-cellular components of inflammation. In the previously mentioned investigation, Amthor and colleagues suggested that the uptake of gadolinium in damaged, necrotic myofibers was conceivably attributed to passive diffusion, not active endocytosis.[25] It is widely accepted that membrane permeability is compromised when myofibers are injured following trauma, thus permitting an influx of extracellular molecules such as albumin. Using albumin as a carrier molecule for uptake of contrast agent into injured muscle fibers is an effective and sensitive way of visualizing skeletal muscle injury, and these results were in close agreement with stereological findings from the TA muscle samples. Collectively, data from Amthor and colleagues,[25] Lovering and colleagues,[22] and the data reported in this investigation demonstrate that following muscle injury the permeability of myofibers is found to increase; we further hypothesize that the concomitant histopathology is related in

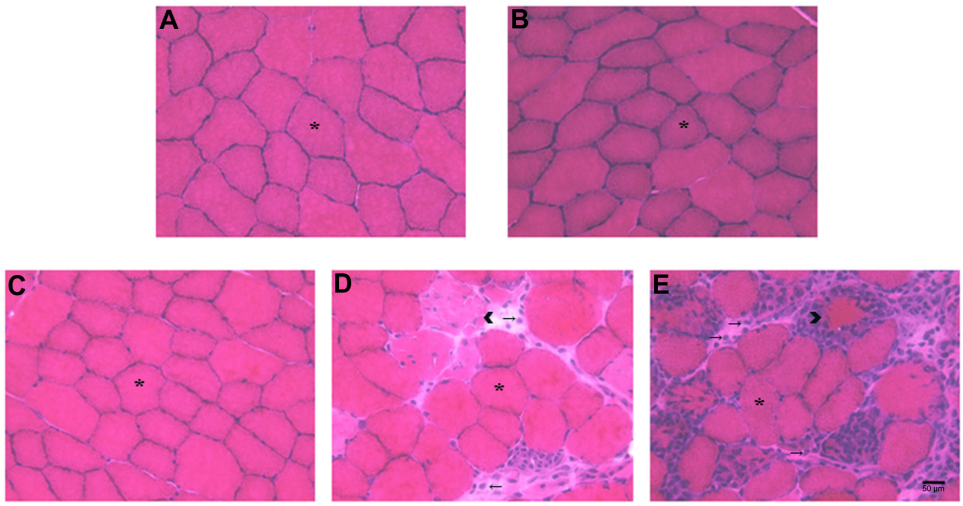

Figure 6. Representative micrographs of TA muscle cross-sections taken at 40× magnification from (**A**) CON, (**B**) isometric contractions, (**C**) 30R, (**D**) 70R, and (**E**) 150R. Asterisks denote normal myofibers, arrow heads denote degenerative myofibers, and arrows denote CI. Scale bar = 50 µm.

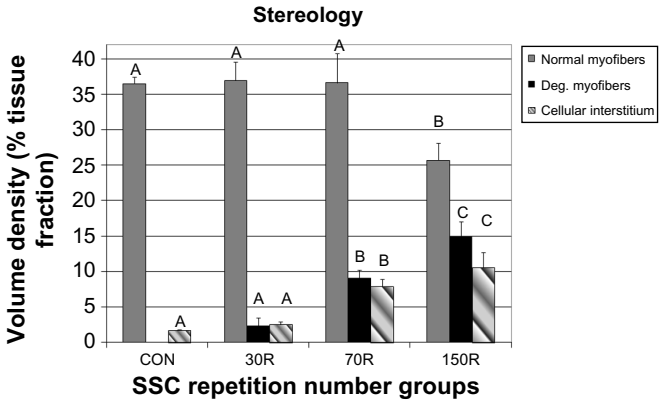

Figure 7. Stereological analyses of the percent volume fraction of normal and degenerative myofibers and CI from TA muscles from animals exposed to 30R, 70R, and 150R as compared to the CON. Comparisons are made between indices, and different letters denote statistical significance at the $P < 0.05$ level (ie, no difference between Cellular Interstitium CON vs. Cellular Interstitium 30R (same letters); difference between Cellular Interstitium 30R vs. Cellular Interstitium 70R vs. Cellular Interstitium 150R. Different letters denote significance [**A** is different from **B** and **C**, **B** is different from **A** and **C**] at the $P < 0.05$ level).

some way to the size (or degree – 1st degree, 2nd degree, or 3rd degree strain – not applicable here as this is a rupture) of the membrane lesion; and that, additionally, depending on the severity of the acute insult, this ultimately leads to overt myofiber degeneration. As such, clinicians routinely use specific modalities (mechanical, electrical, imaging, and/or pharmacological in nature) for intervention and treatment, and would benefit immensely by validating these interventions with the support of evidence-based findings.

Importantly, a limitation of the current study is that it does not utilize standard T1 or T2 imaging, and that the results are specific to the methodology applied in this study. Given that there is question of the accuracy of what exactly the MRI signal intensity represents, our results do suggest that the current methodology is specific and sensitive to the injury inducing exposure as well as quantifying a well-defined temporal recovery point (72 hours) related to peak injury (performance loss and increased histopathological changes), particularly considering that the accompanying histopathology is remarkably consistent and complementary with the current MRI methods utilized. Given that the current investigation is a cross-sectional analysis at three days post injury and that this "snapshot" is quantifying and characterizing an injury and regenerative response accordingly at a single time point, we recognize that future quantitative investigations are needed to complement and advance the current study's findings.

It should be noted that animal models should closely mimic the clinical situation that they intend to characterize, and, as such, our injury paradigm does so by incorporating all of the components of a muscular contraction (isometric, eccentric, and concentric action SSCs). Additionally, and as important, the SSCs utilized here produce a graded effect[6,27] that allows us to investigate different soft-tissue thresholds pertaining to distinct injury states. The results suggest that contrast-enhanced MRI has the sensitivity to differentiate specific degrees of skeletal muscle strain injury, and these non-invasive imaging data are representative of cellular histopathology quantified via invasive, rigorous stereological analyses. Importantly, understanding the exact loading conditions (injurious or overt trauma versus non-injurious or exercise) is paramount to interpretation of the clinical imaging results, especially in the absence of detailed cellular histomorphological data. Specifically, previous investigations have reported that differential MRI findings (ie, T2 values, edema, and total soft-tissue volume) can be associated with the mode of mechanical loading exposure as well as the response in the respective soft tissue (ie, downhill running activity[28] and lengthening-type contractions).[29] Indeed, these investigations have utilized MRI without contrast agents and have reported findings relating to various modes of mechanical loading with diverse responses; and, although the current study's intention was not to evaluate the difference between various MRI methodologies (MRI without contrast agent versus contrast-enhanced MRI), our overall interpretations must be viewed within this context. Nevertheless, our data extend previous research in this area by contributing crucial data that link clinically relevant imaging of soft-tissue injury with physiological events occurring at the cellular level following a physiologically representative *in vivo* model of contraction-induced skeletal muscle injury.

Future investigations will focus on attempting to image regenerative aspects of the biological response following SSC-induced muscle injury impacted by age as well as remodeling events following non-injurious, adaptive SSC loading.[30–34] In conclusion, the current findings have multiple applicable implications and applications across numerous domains (ie, medical, occupational, military, athletic, aging, etc.) involved with musculoskeletal injuries/disorders: (1) provide efficacy for the fundamental differentiation of thresholds of skeletal muscle strain injury (as well as other soft tissues) and the anatomical/cellular representation of the outcomes involved with respect to the clinical manifestation of these conditions, (2) circumvent muscle biopsy, so that a more thorough as well as multiple sampling may be achieved, and, finally, (3) may permit the longitudinal study of skeletal muscle regeneration following injurious events and skeletal muscle remodeling following exercise training.

Acknowledgments

The authors thank Dr. Frank Buczek of the National Institute for Occupational Safety and Health for thorough review and comments concerning the manuscript.

Author Contributions

Conceived and designed the experiments: RGC, GAJ, MSH, BAB. Analyzed the data: RGC, BAB. Wrote the first draft of

the manuscript: RGC, BAB. Contributed to the writing of the manuscript: RGC, GAJ, BAB. Agree with manuscript results and conclusions: RGC, MSH, GAJ, BWJ, SAF, BAB. Jointly developed the structure and arguments for the paper: RGC, MSH, GAJ, BWJ, SAF, BAB. Made critical revisions and approved final version: RGC, MSH, GAJ, BWJ, SAF, BAB. All authors reviewed and approved of the final manuscript.

REFERENCES

1. Garrett WJ. Muscle strain injuries. *Am J Sports Med*. 1996;24:S2–8.
2. Welch LS, Hunting KL, Murawski JA. Occupational injuries among construction workers treated in a major metropolitan emergency department in the United States. *Scand J Work Environ Health*. 2005;31(suppl 2):11–21.
3. Welch LS. Chronic symptoms in construction workers treated for musculoskeletal injuries. *Am J Ind Med*. 1999;36:532–40.
4. Bureau of Labor Statistics (BLS). 2010. Available at http://www.bls.gov/iif/oshdef.htm
5. Avela J, Komi PV. Reduced stretch reflex sensitivity and muscle stiffness after long-lasting stretch-shortening cycle exercise in humans. *Eur J Appl Physiol Occup Physiol*. 1998;78:403–10.
6. Baker BA, Mercer RR, Geronilla KB, Kashon ML, Miller GR, Cutlip RG. Impact of repetition number on muscle performance and histological response. *Med Sci Sports Exerc*. 2007;39:1275–81.
7. Barbe MF, Barr AE. Inflammation and the pathophysiology of work-related musculoskeletal disorders. *Brain Behav Immun*. 2006;20:423–9.
8. Crameri RM, Aagaard P, Qvortrup K, Langerg H, Kjaer M. Myofibre damage in human skeletal muscle: effects of electrical stimulation versus voluntary contraction. *J Physiol*. 2007;583:365–80.
9. Baker BA, Mercer RR, Geronilla KB, Kashon ML, Miller GR, Cutlip RG. Stereological analysis of muscle morphology following exposure to repetitive stretch-shortening cycles in a rat model. *Appl Physiol Nutr Metab*. 2006;31:167–79.
10. Baker BA, Rao KM, Mercer RR, et al. Quantitative histology and MGF gene expression in rats following SSC exercise in vivo. *Med Sci Sports Exerc*. 2006;8:463–71.
11. Geronilla KB, Miller GR, Mowrey KF, et al. Dynamic force responses of skeletal muscle during stretch-shortening cycles. *Eur J Appl Physiol*. 2003;90:144–53.
12. Pizza FX, Peterson JM, Baas JH, Koh TJ. Neutrophils contribute to muscle injury and impair its resolution after lengthening contractions in mice. *J Physiol*. 2005;562:899–913.
13. Lieber RL, Thornell LE, Friden J. Muscle cytoskeletal disruption occurs within the first 15 min of cyclic eccentric contraction. *J Appl Physiol*. 1996;80:278–84.
14. Stauber WT, Smith CA. Cellular responses in exertion-induced skeletal muscle injury. *Mol Cell Biochem*. 1998;179:189–96.
15. Warren GL, Hayes DA, Lowe DA, Armstron RB. Mechanical factors in the initiation of eccentric contraction-induced injury in rat soleus muscle. *J Physiol*. 1993;464:457–75.
16. Cutlip RG, Geronilla KB, Baker BA, et al. Impact of stretch-shortening cycle rest interval on in vivo muscle performance. *Med Sci Sports Exerc*. 2005;37:1345–55.
17. Brooks SV, Zerba E, Faulkner JA. Injury to muscle fibres after single stretches of passive and maximally stimulated muscles in mice. *J Physiol*. 1995;488(pt 2):459–69.
18. Hunter KD, Faulkner JA. Pliometric contraction-induced injury of mouse skeletal muscle: effect of initial length. *J Appl Physiol*. 1997;82:278–83.
19. Clarkson PM, Tremblay I. Exercise-induced muscle damage, repair, and adaptation in humans. *J Appl Physiol*. 1988;65:1–6.
20. Newham DJ, Jones DA, Clarkson PM. Repeated high-force eccentric exercise: effects on muscle pain and damage. *J Appl Physiol*. 1987;63:1381–6.
21. Elsayes K, LammLe M, Shariff A, Totty WG, Habib IF, Rubin DA. Value of magnetic resonance imaging in muscle trauma. *Curr Probl Diagn Radiol*. 2006;35:206–12.
22. Lovering R, McMillan A, Gullapalli R. Location of myofiber damage in skeletal muscle after lengthening contractions. *Muscle Nerve*. 2009;40:589–94.
23. Winkler T, von Roth P, Matziolis G, et al. Time course of skeletal muscle regeneration after severe trauma. *Acta Orthop*. 2011;82:102–11.
24. Cutlip RG, Stauber WT, Willison RH, McIntosh TA, Means KH. Dynamometer for rat plantar flexor muscles in vivo. *Med Biol Eng Comput*. 1997;35:540–3.
25. Amthor H, Egelhof T, McKinnell I, et al. Albumin targeting of damaged muscle fibres in the mdx mouse can be monitored by MRI. *Neuromuscul Disord*. 2004;14:791–6.
26. Underwood EE. *Quantitative Stereology*. Reading, MA: Addison-Wesley Publishing Co; 1970:23–34.
27. Hesselink MK, Kuipers H, Geurten P, Van Straaten H. Structural muscle damage and muscle strength after incremental number of isometric and forced lengthening contractions. *J Muscle Res Cell Motil*. 1996;17:335–41.
28. Marqueste T, Giannesini B, Fur YL, Cozzone PJ, Bendahan D. Comparative MRI analysis of T2 changes associated with single and repeated bouts of downhill running leading to eccentric-induced muscle damage. *J Appl Physiol*. 2008;105:299–307.
29. Foley JM, Jayaraman RC, Prior BM, Pivarnik JM, Meyer RA. MR measurements of muscle damage and adaptation after eccentric exercise. *J Appl Physiol*. 1999;87(6):2311–8.
30. Baker BA, Hollander MS, Kashon ML, Cutlip RG. Effects of glutathione depletion and age on skeletal muscle performance and morphology following chronic stretch-shortening contraction exposure. *Eur J Appl Physiol*. 2010;108:619–30.
31. Hollander MS, Baker BA, Ensey J, Kashon ML, Cutlip RG. Effects of age and glutathione levels on oxidative stress in rats after chronic exposure to stretch-shortening contractions. *Eur J Appl Physiol*. 2010;105:589–97.
32. Ryan MJ, Dudash HJ, Docherty M, et al. Vitamin E and C supplementation reduces oxidative stress, improves antioxidant enzymes and positive muscle work in chronically loaded muscles of aged rats. *Exp Gerontol*. 2010;45:882–95.
33. Ryan MJ, Dudash HJ, Docherty M, et al. Aging-dependent regulation of antioxidant enzymes and redox status in chronically loaded rat dorsiflexor muscles. *J Gerontol A Biol Sci Med Sci*. 2008;63 A(10):1015–26.
34. Cutlip RG, Baker BA, Geronilla KB, et al. Chronic exposure to stretch-shortening contractions results in skeletal muscle adaptation in young rats and maladaptation in old rats. *Appl Physiol Nutr Metab*. 2006;31:573–87.
35. Baker BA, Cutlip RG. Skeletal muscle injury versus adaptation with aging: novel insights on perplexing paradigms. *Exerc Sport Sci Rev*. 2010;38:10–6.
36. Cutlip RG, Baker BA, Hollander M, Ensey J. Injury and adaptive mechanisms in skeletal muscle. *J Electromyogr Kinesiol*. 2009;19:358–72.